ARMY RESEARCH LABORATORY

Dynamic Evaluation of Acrylonitrile Butadiene Styrene Subjected to High-Strain-Rate Compressive Loads

by Alex Peterson, Ed Habtour, Jaret Riddick, Michael Coatney, Denzell Bolling, and Gbadebo Owolabi

ARL-TN-0648 **December 2014**

NOTICES

Disclaimers

The findings in this report are not to be construed as an official Department of the Army position unless so designated by other authorized documents.

Citation of manufacturer's or trade names does not constitute an official endorsement or approval of the use thereof.

Destroy this report when it is no longer needed. Do not return it to the originator.

Army Research Laboratory
Aberdeen Proving Ground, MD 21005-5066

ARL-TN-0648 **December 2014**

Dynamic Evaluation of Acrylonitrile Butadiene Styrene Subjected to High-Strain-Rate Compressive Loads

Alex Peterson, Denzell Bolling, and Gbadebo Owolabi
Department of Mechanical Engineering, Howard University

Ed Habtour, Jaret Riddick, and Michael Coatney
Vehicle Technology Directorate, ARL

REPORT DOCUMENTATION PAGE	Form Approved OMB No. 0704-0188

1. REPORT DATE *(DD-MM-YYYY)*	2. REPORT TYPE	3. DATES COVERED (From – To)
December 2014	Final	1 June 2013–31 August 2013

4. TITLE AND SUBTITLE
Dynamic Evaluation of Acrylonitrile Butadiene Styrene Subjected to High-Strain-Rate Compressive Loads

5a. CONTRACT NUMBER

5b. GRANT NUMBER

5c. PROGRAM ELEMENT NUMBER

6. AUTHOR(S)
Alex Peterson, Ed Habtour, Jaret Riddick, Michael Coatney, Denzell Bolling, and Gbadebo Owolabi

5d. PROJECT NUMBER

5e. TASK NUMBER

5f. WORK UNIT NUMBER

7. PERFORMING ORGANIZATION NAME(S) AND ADDRESS(ES)
U.S. Army Research Laboratory
ATTN: RDRL-VTD
Aberdeen Proving Ground, MD 21005-5066

8. PERFORMING ORGANIZATION REPORT NUMBER
ARL-TN-0648

9. SPONSORING/MONITORING AGENCY NAME(S) AND ADDRESS(ES)

10. SPONSOR/MONITOR'S ACRONYM(S)

11. SPONSOR/MONITOR'S REPORT NUMBER(S)

12. DISTRIBUTION/AVAILABILITY STATEMENT
Approved for public release; distribution is unlimited.

13. SUPPLEMENTARY NOTES

14. ABSTRACT
The current goal of the investigation is to understand the potential energy absorption benefits of components fabricated using fused deposition modeling additive manufacturing. Tensile test specimens were fabricated according to the ASTM D 638 standard to characterize the general mechanical behavior of the three-dimensional–printed acrylonitrile butadiene styrene (ABS) material to assess potential strain-rate dependency. The dynamic responses were also necessary to characterize the dynamic evolution of ABS in compression at various strain rates. The ABS specimens were subjected to high-strain-rate deformation using the split-Hopkinson pressure bar. A new phenomenon, described as a multistage collapse in which the samples undergo multiple stages of compression and expansion, was observed during compression. As the velocity increased, the capability for energy absorption decreased to where there was only one stage of compression equivalent to the initial stage.

15. SUBJECT TERMS
high strain rate, acrylonitrile, butadiene, styrene, 3-D printed, split-Hopkinson, direct digital manufacturing

16. SECURITY CLASSIFICATION OF:			17. LIMITATION OF ABSTRACT	18. NUMBEROF PAGES	19a. NAME OF RESPONSIBLE PERSON
a. REPORT	b. ABSTRACT	c. THIS PAGE			Michael Coatney
Unclassified	Unclassified	Unclassified	UU	20	19b. TELEPHONE NUMBER (*Include area code*) 410-278-9834

Standard Form 298 (Rev. 8/98)
Prescribed by ANSI Std. Z39.18

Contents

List of Figures

List of Tables

1. Introduction

Direct digital manufacturing (DDM), commonly known as additive manufacturing (AM), uses various thermoplastics to create models that are printed for a vast amount of applications. These applications could be potentially beneficial with respect to mechanical and structural designs. Acrylonitrile butadiene styrene (ABS) can be printed at various orientations using this approach. Further understanding of the effect that the DDM process provides could lead to potential benefits that were previously unexplored. DDM uses a combination of computer-aided design (CAD) and computer-aided manufacturing (CAM), as well as computer codes designed to interface with advanced three-dimensional (3-D) additive manufacturing prototyping machines, to produce a design (*1*). Riddick et al. (*2*) observed that building in the horizontal direction with a 0° rotation achieved the highest tensile strength (32.60 MPa). Table 1 describes the mechanical results from different build directions and their corresponding orientations.

Table 1. Build orientation response: ASTM 638 test results for ABS specimens using fused deposition modeling (*3*).

Build Direction	Raster Orientation	Poisson's Ratio	Tensile Strength (MPa)	Tensile Modulus (GPa)
Horizontal	0°	0.374	32.60	2.69
	90°	0.360	15.26	2.45
	0°/90°	0.371	25.69	2.59
Side	0°	0.386	34.17	2.79
	90°	0.372	24.24	2.53
	0°/90°	0.373	29.11	2.65
Vertical	0°	0.329	4.57	2.45
	90°	0.349	15.30	2.40
	0°/90°	0.321	8.56	2.31

Advanced 3-D additive manufacturing prototyping (3-D printing) has been used in a variety of applications, which include medical designs, oil filter assemblies, prototypes, replacement parts, and dental crowns (*4*). This study explores the fused deposition modeling (FDM) and the printing orientation as a means to quantify the potential benefits. These benefits include more cost-effective, time-efficient, in-house fabrication of designs, while optimizing the mechanical and structural integrity. In FDM, CAD software is used to convert a file containing a 3-D model into 3-D stereolithography (STL) format. The STL file is imported into CAM software, which produces a physical replica of the 3-D model that is sliced into thin layers composed of tool paths. The 3-D printing machine uses these tool paths to place continuous feedstock filament onto a surface, thus building it up the 3-D component layer by layer (*2*).

In the design of mechanical and structural components, it is essential to understand the mechanical behavior at different loading rates based on the required design. The present investigation aims at understanding the effect of high-strain-rate loading (greater than 10^2 s^{-1}) on various forms of ABS for potential benefits in energy absorption, as well as mechanical and structural applications. In the area of high-strain-rate deformation, there has been extensive work on understanding the effects of high strain rate on metals such as aluminum alloys, steels and other metals (*5*–*8*). Limited exploratory research has been conducted in the area of plastics, more specifically ABS. Many experiments were conducted through use of the split-Hopkinson pressure bar (SHPB) for strain rates greater than 10^2 (*3*). The range of interest for the present study (10^2–10^3) fell squarely within the capability of the SHPB test apparatus making this setup suitable for completing the experiments required to investigate the dynamic evolution of ABS.

Distorted grain regions that are associated with large amounts of shear characterize deformed bands. They are also known to be harder and more brittle than the more frequently observed in hardened steels (*9*). One main relationship that is analyzed when observing metals at high strain rates is the relationship between the stresses the material undergoes as the strain is increased. Lee et al. (*10*), Qiang et al. (*11*), and Yazdani et al. (*12*) conducted studies for observing the dynamic deformation of copper and titanium alloys and observed that the maximum stress at these high strain rates did not drastically change relative to surrounding strain rates. Siviour et al. (*13*) showed that the final strain achieved for polymers was directly related to the strain rate applied along with its relationship to the stress experienced in a material at high-strain-rate deformation.

For polymers such as ABS, the mechanical properties vary considerably from those observed in metals. Knowledge of the strain-rate dependency of ABS will help determine what the stress limits are due to the required design application as a function of the strain rate. One of the limited studies for characterizing the strain-rate dependency of polymers was performed by Mulliken and Boyce (*14*), where they investigated the strain-rate dependency of glassy polymers from 10^{-4} to 10^4 s^{-1}. They were able to demonstrate that an increase in strain-rate sensitivity was observed at elevated loading rates compared to those observed at quasi-static loading. Walley and Field (*15*) conducted multiple tests on the strain-rate sensitivity of polymers subjected to loads ranging from quasi-static to high strain rates. They fabricated samples using solid ABS block to determine the mechanical properties of ABS at various strain rates The novelty of the present research is that rather than testing a solid block of ABS machined down to the appropriate size, an advanced 3-D additive manufacturing approach is used to create highly optimized logical structures for energy absorption.

Through the analysis of solid ABS, a linear relationship between the strain rate applied and the maximum stress observed in the quasi-static region was noted (*15*). As the transitional phase from quasi-static to dynamic loading is entered, there is a drastic change in the increase in the gradient of the slope. Unlike observations of adiabatic conditions occurring with metals, there is

no drastic change in temperature. Understanding whether the potential benefits of a 3-D printed polymer can be harnessed for use in highly optimized and multifunctional mechanical and structural applications is important.

2. Experimental Approach

Before experiments at high strain rates were conducted, it was essential to understand how the material would behave under quasi-static loading conditions. This interest arises from the fact that most polymers are strain-rate sensitive, i.e., the maximum stress observed in an object before deformation, or failure, is directly related to the rate of strain being applied to the material. Over a wide range of strain rates there were different levels of maximum stress observed in the ABS throughout the experiments. To understand the tensile properties of the 3-D printed ABS, preliminary tensile tests were conducted using the ASTM D 638-03 Standard Test Method for Tensile Properties of Plastics. The standard recommends a Type I specimen for rigid and semirigid plastics (*16*). Tensile testing was prescribed at a rate of 5 mm/min. Type I specimen dimensions used in the tensile testing are shown in figure 1.

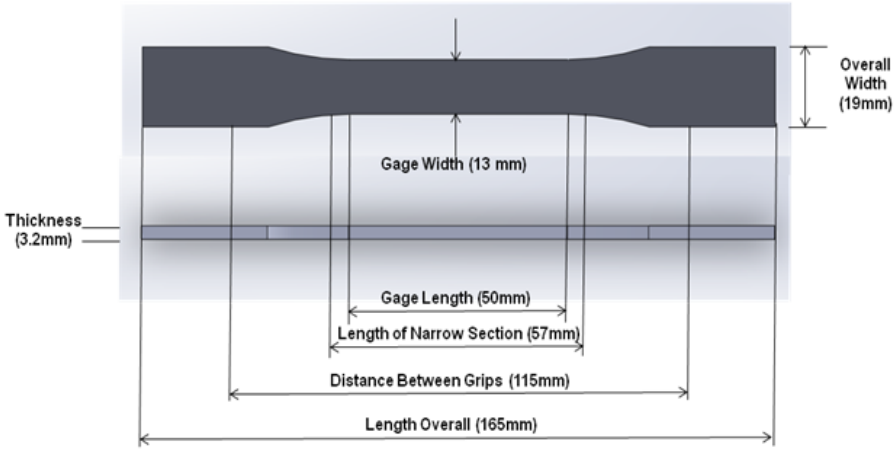

Figure 1. ASTM D 638-03 dog bone.

When designing the specimen for tensile testing, it is important that the tensile specimen be built such that the orientation of the tensile test loads corresponds to the subsequent dynamic tests. The tensile specimen was built with each successive layer composed of 0° and 90° orientations built from the ground up, as shown in figure 2. According to the ASTM D 638-03 standard (*16*), the test specimen is to be tested at minimum of 0.50 cm/min to extract material properties such as yield point, elastic modulus, and ultimate tensile strength. To understand if the material was strain-rate dependent, experiments were performed at displacement rates of 0.5, 5, 25, 35, and 50 cm/min. Figures 3 and 4 show the specimen before and after testing was conducted.

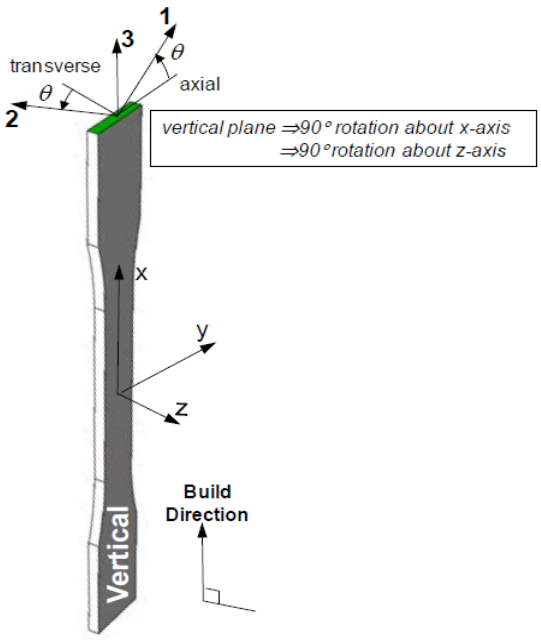

Figure 2. Material build direction 0°/90° orientation.

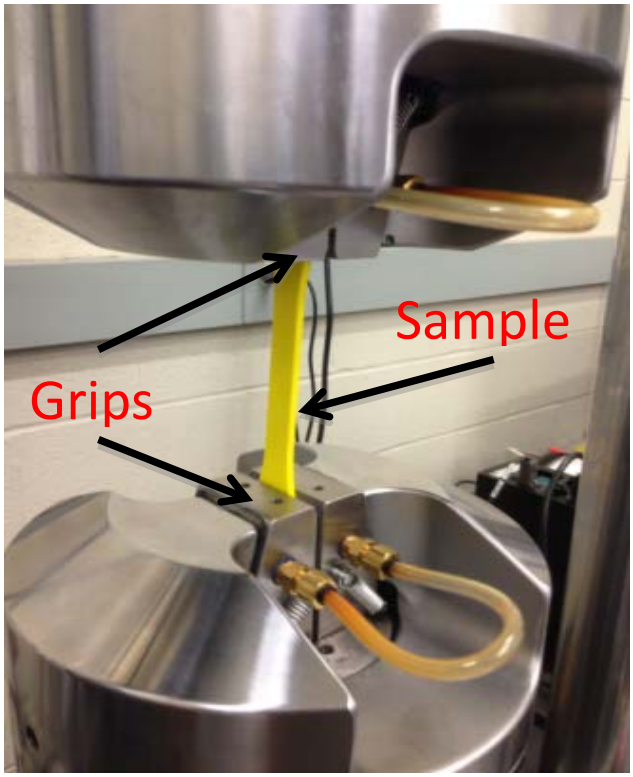

Figure 3. Experimental setup prior to testing.

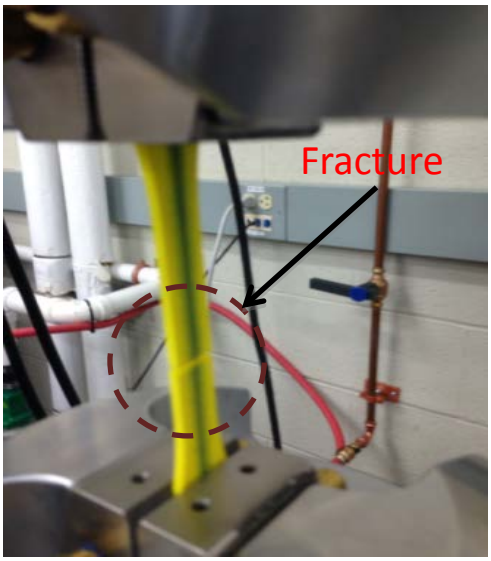

Figure 4. Experimental setup after testing.

Once the tensile testing was completed, the next phase in the material design and testing was the uniaxial compression loading at high strain rates. The specimens for compression were 8 mm long and 8 mm in diameter. The compressive loading was conducted using the conventional Split–Hopkinson Pressure Bar. The setup was composed of a gas gun connected to a striker bar that induced a velocity into the system. The velocity was then transferred to an incident bar that had a strain gauge attached to it to capture the dynamic response as a result of the applied compression on the specimen. The reflected waves from the specimen were captured through the same strain gauge that recorded the incident waves. On the other side of the specimen was the transmitted bar, which captured the waves that were transmitted through the specimen as a result of the compressive loading. The measurements were then relayed from the strain gauge to an oscilloscope, which provided the output signals. The signals were converted into time-domain stress, strain, velocity, displacement, force, and strain rate (*17*). Finally, these properties were observed to consider the effects of dynamic loading on the ABS cylindrical specimen. In conjunction with the data captured by strain gages and oscilloscope, the material deformation was also captured by utilizing a high speed digital image correlation (DIC) system, which captured the compression at 124,000 frames per second (fps). The DIC code developed by ARAMIS was utilized to capture the movement of certain points along the load axis as a result of deformation by tracking dots that were applied through spray painting patterns of black and white along the length of the specimen. A comparison between 8-mm plain and spray-painted specimen is shown in figure 5.

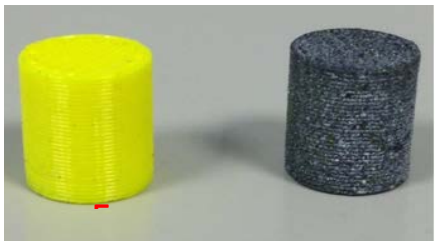

Figure 5. (a) Unpainted specimen (b) painted specimen.

3. Results and Discussion

Testing the ABS specimen was accomplished in two different stages. The first stage was tensile testing to further understand the possibility of strain-rate dependency for the ABS tested as well as the maximum stress observed to allow for calculating values of the strain rate. For the second stage high-strain-rate tests, the ABS samples were tested at strain rates from 500 to 2000 s^{-1}.

3.1 Material Characterization

The 3-D printed ABS material was brittle, and therefore, no evidence of plastic deformation was apparent in the tensile experiments, which was directly related to the manner in which the material was built. Figure 6 shows the stress strain curve from the tensile testing at various displacement rates. Table 2 shows the specimen testing rates for strain-rate dependency.

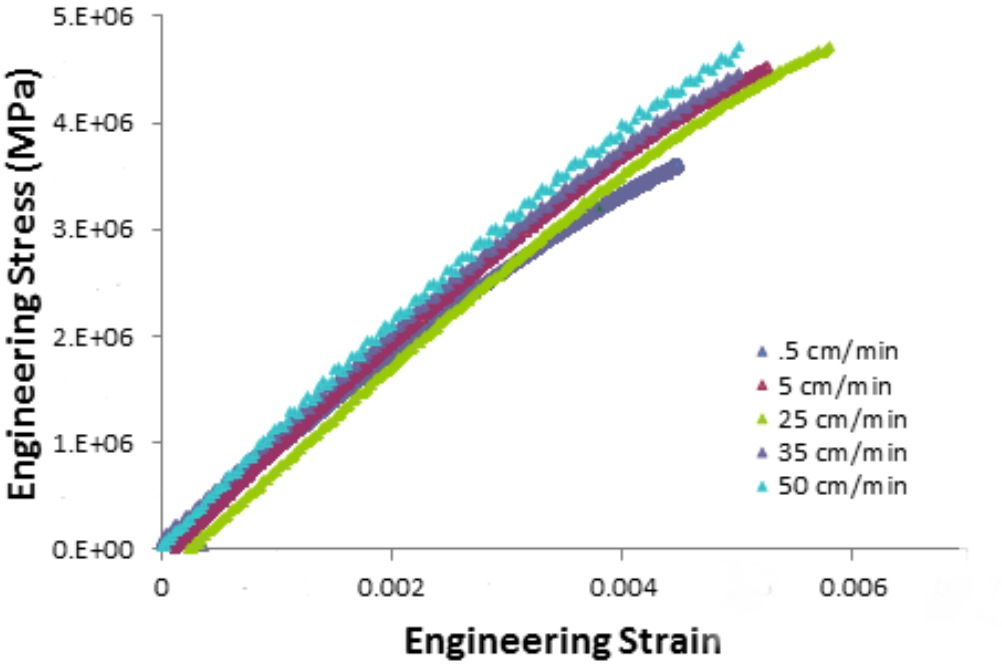

Figure 6. Stresses, strain tensile results.

Table 2. Tensile testing results.

Displacement Rate (cm/min)	Value
0.5	1.0
5	0.9
25	1.0
50	1.0
Average = 0.975	

At the initial strain rate, the stress observed in the system was 3.4 MPa, which was the lowest out of the five stress results observed. However, the modulus of elasticity appeared to be consistent among the specimens. As the load rate was increased from 0.5 cm/min to 50 cm/min, the stresses of the specimen are around the same levels as well as the maximum strain experienced before failure occurs.

Using these results, the maximum stress was applied to calculations relating for the bar properties and applied pressure to capture various strain rates based on the specimen size. From these calculations, a relationship between material properties, strain rate, velocity, and tank pressure are established (as seen in table 3).

Table 3. Strain rate, pressure, and velocity relationship.

ABS 8 × 8 mm^2 Cylindrical Specimen			ABS 10 × 10 mm^2 Cylindrical Specimen		
Strain Rate (s^{-1})	Velocity (m/s)	Pressure (kPa)	Strain Rate (s^{-1})	Velocity (m/s)	Pressure (kPa)
500	4.096	20.68	500	5.154	26.82
750	6.097	32.96	750	7.656	44.61
1000	8.097	48.33	1000	10.158	68.19
1500	12.097	91.08	1500	15.162	114.80
2000	16.098	150.86	2000	20.165	224.84

3.2 Compression Analysis

The experimental results showed that at lower strain rates there were different stages of deformation observed while the specimen underwent one initial impact. Figure 7 shows the deformation observed due to compression with respect to time, where Y is the longitudinal displacement.

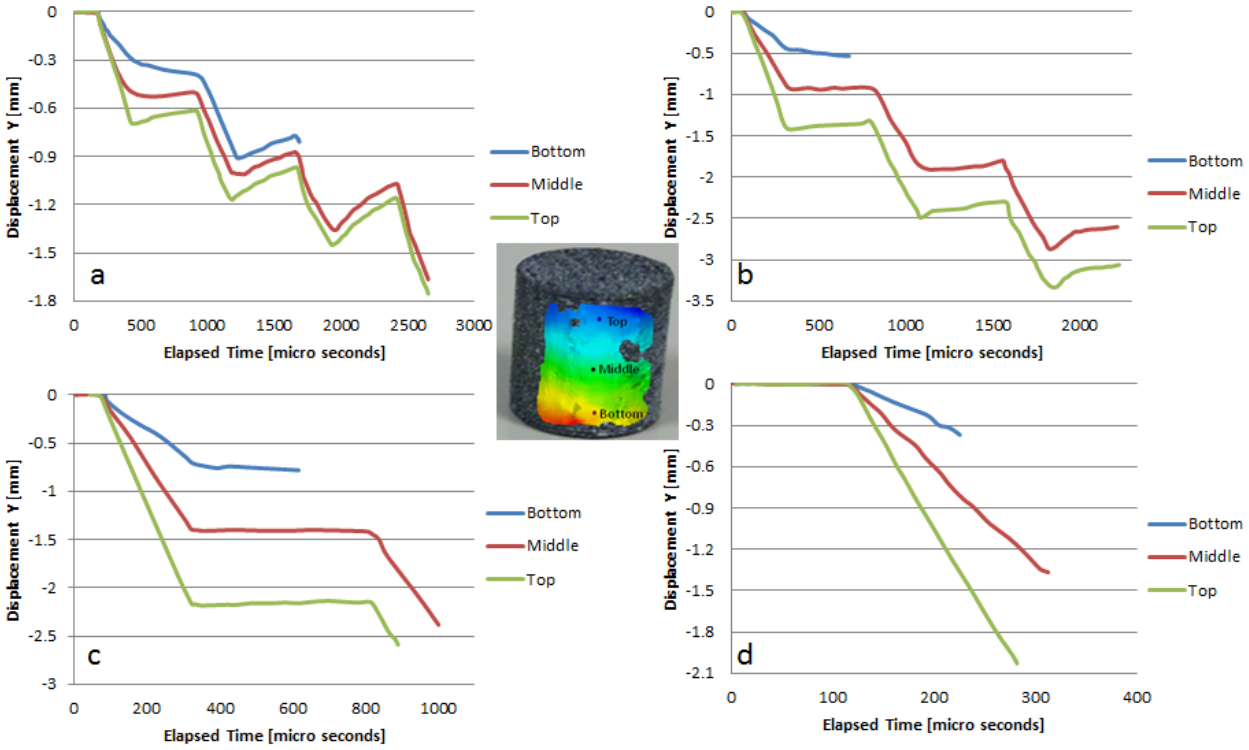

Figure 7. Longitudinal stage displacement: (a) 500 s^{-1}, (b) 1000 s^{-1}, (c) 1500 s^{-1}, and (d) 2000 s^{-1}.

Using the DIC, three different points throughout the material were captured and analyzed as the specimen went under compression, as shown in figure 7. Top, middle, and bottom location reference points on the specimen were provided in figure 7. These points were selected to characterize the dynamic response of the samples at different stages. At a strain rate of 500 s^{-1}, as shown in figure 7a, compression was not evident until about 200 µs, as shown in figure 7a. Beyond this stage, however, the compression began and the specimen contracted longitudinally. Toward the end of this stage, the material expanded slightly and the overall displacement increased until the next stage of contractions occurred. As the induced strain rate increased, the stages of deformation decreased until eventually there was only one stage at 2000 s^{-1}, as shown in figures 7b–7d. The displacements observed by the system were also evident in the compression video captured by the high speed camera. The phenomenon is believed to be a function of the support ring built around the 3-D printed material, which holds the perpendicular layers in place, as it begins to absorb and displace energy acting as a multistage spring. Once the outer ring reached its maximum limit of energy absorption, it collapsed and the energy was transferred to the perpendicular layers causing a complete fracture of the sample at 2000 s^{-1}.

Table 4 shows the initial height of the specimen before deformation in comparison to the final height. Interestingly, at the lowest strain rate displayed (500 s^{-1}), the specimen showed signs of actually expanding after the compression process was completed. When the strain rate reached

750 s^{-1}, the average final height began to gradually decrease. At this strain rate and higher, failure began to occur by buckling until complete fracture was observed. At a strain rate of 2000 s^{-1}, the specimen size reduced to approximately 60% and specimen fracture occurred.

Table 4. Specimen height comparison.

Strain Rate (s^{-1})	Initial Height (mm)	Average Final Height (mm)
500	8	8.11
750	8	7.95
1000	8	7.18
1500	8	5.85
2000	8	4.07

The damage evolution of the specimen started to become drastic once the applied strain rate exceeded 1000 s^{-1}, as shown in figure 8; these images are of the specimens after testing.

Figure 8. Specimen deformation.

The specimen failure as a function of the strain rate can be divided into two different regions, the first consisting of 500–1000 s^{-1} and the second consisting of the final two strain rates, 1500 s^{-1} and 2000 s^{-1} (as shown in figure 9). Each of these specimens underwent multiple stages of stress increase and stress decrease, but as the strain rate increased, the differences became less drastic in region 1. As the transition from region 1 to region 2 occurred, the corresponding yield point changed along with the maximum stress. For a strain rate of 1500 s^{-1}, the yield point and the maximum stress were 91.64 and 93.06 MPa, respectively. For the strain rate of 2000 s^{-1}, yielding occurred at 89.67 MPa and the maximum stress was 96.67 MPa. In this region, there was one significant drop in stress, an increase in stress, and then a drastic decrease as a result of stress collapse.

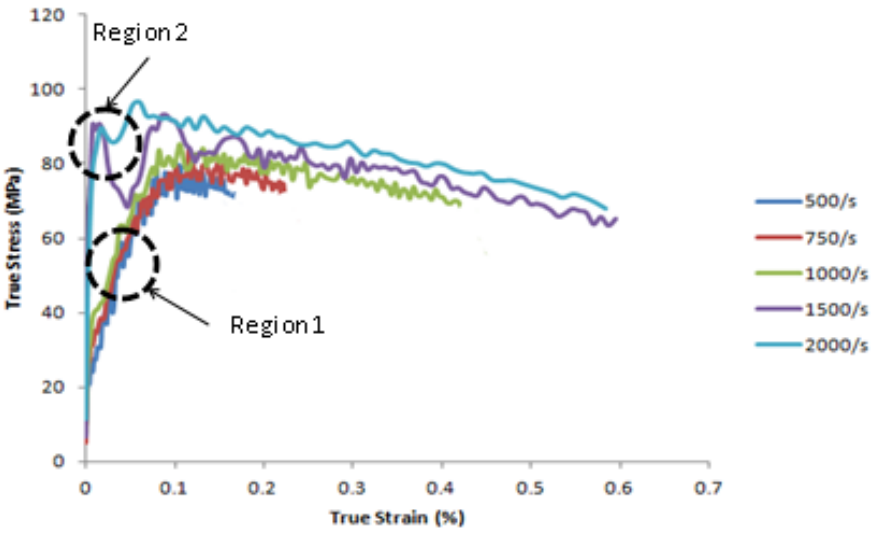

Figure 9. Stress strain curve.

4. Conclusions

Throughout this research, exploratory studies have been conducted in understanding the effect of the 3-D printing on the response of ABS polymer. At strain rates above 1000 s^{-1} failure begins to occur in the printed ABS by buckling, where as below this there is minimal height reduction and failure observed. At the lower strain rates from images captured through the use of the DIC system, there is some contraction and expansion of the material evident. This is believed to be a result of the ring that is built around the specimen holding the perpendicular layers in place absorbing the energy acting as a multi-stage spring, which results in the compression and expansion of the specimen in the longitudinal.

The specimen expresses a linear relationship between stress and strain up until it its reaches its yield point. More plastic deformation is observed at higher strain rates along with higher levels of stress. However, as the strain rate is increased there is a more evident showing of stress collapse ultimately leading to the failure of the specimen. While ABS does not display stress limits in the dynamic response similar to those seen in metals, the multistage collapse indicates a potential for novel energy absorption mechanism to be exploited at lower strain rates. Future work in the area should include more studies about printing orientation as well as investigating the impact of the presence of the outer cylindrical ring on the overall dynamic response.

5. References

1. Odeshi, A. G.; Bassim, M. N.; Al-Ameeri, S.; Li, Q. Dynamic Shear Band Propagation and Failure in AISI 4340 Steel. *J. Materials Processing Technology* **2005,** *169* (2), 150–155.
2. Riddick, J. C.; Hall, A. J.; Haile, M. A.; Von Wahlde, R.; Cole, D. P.; Biggs S. J. Effect of Manufacturing Parameters on Failure in Acrylonitrile-Butadiane-Styrene Fabrication Fused Deposition Modeling. *Proceedings of the 53rd AIAA/ASME/ASCE/AHS/ASC Structures, Structural Dynamics and Materials Conference*, Honolulu, HI, 23–26 April 2012.
3. Kuhn, H.; Medlin, D. *ASM Handbook: Volume 8: Mechanical Testing and Evaluation;* The Materials Information Society: Materials Park, OH, 2000; pp. 462–476.
4. Berman, B. 3-D Printing: The New Industrial Revolution. *Business Horizons* **2012,** *55* (2), 155–162.
5. Smerd, R.; Winkler, S.; Salisbury, C.; Worswick, M.; Lloyd, D.; Finn, M. High Strain Rate Tensile Testing of Automotive Aluminum Alloy Sheet. *International J. Impact Engineering* **December 2005,** *32* (1–4), 541–560.
6. Djapic Oosterkamp, L.; Ivankovic, A.; Venizelos, G. High Strain Rate Properties of Selected Aluminium Alloys. *Materials Science and Engineering: A* **2000,** *278* (1–2), 225–235.
7. Odeshi, A. G.; Al-ameeri, S.; Mirfakhraei, S.; Yazdani, F.; Bassim, M. N. Deformation and Failure Mechanism in AISI 4340 Steel Under Ballistic Impact. *Theoretical and Applied Fracture Mechanics* **2006,** *45* (1), 18–24.
8. Lee, W. S.; Lin, C. F. Plastic Deformation and Fracture Behaviour of Ti–6Al–4V Alloy Loaded With High Strain Rate Under Various Temperatures. *Materials Science and Engineering: A* **1998,** *241* (1–2), 48–59.
9. Ghomi, H. M. Adiabatic Shear Localization in AISI 1340 and 4340 Steels: The Influence of Microstructure and Geometry. Master's Thesis, University of Saskatchewan, Saskatoon, Saskatchewan, Canada, 2011.
10. Lee, D. G.; Kim, Y. G.; Nam, D. H.; Hur, S. M.; Lee, S. Dynamic Deformation Behavior and Ballistic Performance of Ti–6Al–4V alloy Containing Fine α2 (Ti3Al) Precipitates. *Materials Science and Engineering: A* **2005,** *391* (1–2), 221–234.
11. Qiang, L.; Yongbo, X.; Bassim, M. N. Dynamic Mechanical Properties in Relation to Adiabatic Shear Band Formation in Titanium Alloy-Ti17 *Materials Science and Engineering: A* **2003,** *358* (1–2), 128–133.

12. Yazdani, F.; Bassim, M. N.; Odeshi, A. G. The Formation of Adiabatic Shear Bands in Copper During Torsion at High Strain Rates. *Procedia Engineering* **2009,** *1* (1), 225–228.

13. Siviour, C. R.; Walley, S. M.; Proud, W. G.; Field, J. E. Mechanical Behaviour of Polymers at High Rates of Strain. *Journal De Physique IV* **2006,** *134*, 949–955.

14. Mulliken, A. D.; Boyce, M. C. Mechanics of the Rate-Dependent Elastic–Plastic Deformation of Glassy Polymers From Low to High Strain Rates. *International Journal of Solids and Structures* **2006,** *43* (5), 1331–1356.

15. Walley, S. M.; Field, J. E. Strain Rate Sensitivity of Polymers in Compression from Low to High Rates. *Dymat Journal* **1994,** *1*, 211–227.

16. ASTM D 638-03. International, Standard Test Method for Tensile Properties of Plastics *Annu. Book ASTM Stand.* **2004,** 1–15.

17. Zukas, J. *High Velocity Impact Dynamics;* John Wiley & Sons, Inc.: New York 1990.

18. Odoh, D. Full Field Measurement of the Dynamic Response of AA6061-T6 Aluminum Alloy Under High Strain Rate Compression and Torsion Loads. Thesis, Howard University, Washington, DC, 2012.

1 (PDF) DEFENSE TECHNICAL INFORMATION CTR DTIC OCA

2 (PDF) DIRECTOR US ARMY RESEARCH LAB RDRL CIO LL IMAL HRA MAIL & RECORDS MGMT

1 (PDF) GOVT PRINTG OFC A MALHOTRA

1 (PDF) DIR USARL RDRL VTM M COATNEY

INTENTIONALLY LEFT BLANK.